LOW FREQUENCY ERROR ANALYSIS AND CALIBRATION FOR HIGH-RESOLUTION OPTICAL SATELLITE'S UNCONTROLLED GEOMETRIC POSITIONING

Mi Wang[a], Chengcheng Fan[a,*], Bo Yang[b], Yufeng Cheng[a]

[a] State Key Laboratory of Information Engineering in Surveying, Mapping and Remote Sensing, Wuhan University, Wuhan 430079, China – wangmi@whu.edu.cn ; ccfan@whu.edu.cn ; cyf_whu@126.com
[b] Collaborative Innovation Center of Geospatial Technology, Wuhan University, Wuhan 430079, China - 2009106190044@whu.edu.cn

Commission I, WG I/4

KEY WORDS: high-resolution optical satellite; low frequency error; star sensor; uncontrolled geometric positioning

ABSTRACT:

The low frequency error is a key factor which has affected uncontrolled geometry processing accuracy of the high-resolution optical image. To guarantee the geometric quality of imagery, this paper presents an on-orbit calibration method for the low frequency error based on geometric calibration field. Firstly, we introduce the overall flow of low frequency error on-orbit analysis and calibration, which includes optical axis angle variation detection of star sensor, relative calibration among star sensors, multi-star sensor information fusion, low frequency error model construction and verification. Secondly, we use optical axis angle change detection method to analyze the law of low frequency error variation. Thirdly, we respectively use the method of relative calibration and information fusion among star sensors to realize the datum unity and high precision attitude output. Finally, we realize the low frequency error model construction and optimal estimation of model parameters based on DEM/DOM of geometric calibration field. To evaluate the performance of the proposed calibration method, a certain type satellite's real data is used. Test results demonstrate that the calibration model in this paper can well describe the law of the low frequency error variation. The uncontrolled geometric positioning accuracy of the high-resolution optical image in the WGS-84 Coordinate Systems is obviously improved after the step-wise calibration.

1. INTRODUCTION

Geometric positioning accuracy of high-resolution optical satellite images without control points depends on satellite orbit accuracy determined by GPS, time synchronization accuracy between each payload, the relative installation parameters accuracy between each payload, internal calibration accuracy of earth observation camera, attitude determination accuracy based on star sensor and gyro combination and other factors (Tang et al., 2011; Li et al., 2016). Among them, the low frequency error of star sensor, mounting structure change caused by space thermal environment as well as attitude datum changes caused by different star sensor mode switching are import factors restricting the high-precision geometry processing of optical remote sensing image (Jin et al., 2013).

Due to the factors of alternating hot and cold space environment and field of view changes, the space-borne star sensor will generate an error by cyclical changes in the orbital period, that star sensor low frequency error, which is one of the important components of star sensor's measurement error, difficult to be eliminated by a general filtering method, and it is important factor causing low frequency error (Xiong et al., 2014). While periodically changing angles by the sun, resulting in uneven heating of the overall structure of the satellite and cyclical changes of relative installation parameters between payloads, which will always cause low frequency error. For the presence of low frequency error in the satellite image geometry processing, domestic and foreign scholars have carried out related research. The related literatures have carried on the analysis to the error source of optical image geometric processing, influence degree of different types of errors and solution method, proposed orbit calibration of payloads installation errors and internal camera distortion based on geometric calibration field (Yuan, 2012; Bouillon, 2006; Wang,

2012). There are some other literatures did research on the error source of on-board star sensors, and put forward taking star sensor's low frequency error parameter expansion as a state. It combined the satellite attitude kinematics model and low frequency error mathematical model, designed extension kalman filter, estimated the satellite attitude, gyro drift and star sensor's low-frequency error parameters (Sun, 2013; Liu, 2009; Wang, 2012; Xiong, 2014). In summary, the above research work is mainly based on the star sensor's own observation information for low frequency error calibration, due to the lack of absolute attitude reference, it is difficult to effectively eliminate the low frequency error. At the same time, the influence of installation parameter variation and attitude datum changes caused by different star sensor switching on the geometric accuracy of the image is not yet seen in the existing literature.

In this paper, a model based on fourier series was proposed for modelling and compensating the low frequency error in image geometry processing. The data of a certain type of high resolution optical satellite launched in July 2015 was analysed, and the geometric calibration field was used to verify and evaluate the algorithm in this paper.

2. LOW FREQUENCY ERROR COMPENSATION BASED ON FOURIER SERIES MODEL

2.1 The method

To effectively eliminate or weaken the influence of low frequency error on image geometric positioning accuracy under no control point, this paper proposed ground compensation method, including the following specific processes:
(1) Low frequency error analysis and detection based on optical axis angle change between the star sensors.

(2) Achieving high accuracy of internal datum unifying based on multi-star sensor relative calibration.
(3) Precision attitude inversion of camera based on geometric calibration field.
(4) Absolute calibration of external datum.

2.2 Internal datum calibration and unifying

High resolution optical satellite usually configures three star sensors, and we could determine the absolute satellite attitude information based on the optical axis vectors of two star sensors. The three star sensors are identified as A, B, C, and any of the two star sensors combination can be used to get the absolute attitude of three different datum. By the thermal deformation of the satellite overall structure and star sensor's low frequency error, the conversion between the three different datum is not a constant value, is a time varying system error, need modeling calibration. Three datum coordinates are defined as AB, AC, BC virtual body coordinate system. With BC and AB two combination mode as an example, the absolute attitudes of AB combination mode and BC combination mode are aligned with the time scale, and further we could calculate the conversion parameters between AB and BC datum based on the following methods. Suppose the absolute attitude quaternion of AB and BC combination models at a certain time t_k are that:

$$q_t^{AB} = \begin{bmatrix} q_{0AB} & q_{1AB} & q_{2AB} & q_{3AB} \end{bmatrix}^T,$$

$q_t^{BC} = \begin{bmatrix} q_{0BC} & q_{1BC} & q_{2BC} & q_{3BC} \end{bmatrix}^T$, and we could get

the rotation matrix R_{AB}^I, R_{BC}^I of body to J2000 coordinate system at time t_k. Next, the conversion matrix $R_{AB}^{BC} = (R_{BC}^I)^T R_{AB}^I$ and Euler angle conversion parameters $\Delta_{AB}^{BC} = \begin{bmatrix} \Delta_{\psi,k} & \Delta_{\varphi,k} & \Delta_{\theta,k} \end{bmatrix}^T$ of AB datum to BC datum are obtained, and we could get sequence of low frequency error when the multi-cycle data are processed according to the method.

Considering the low frequency error is periodic signal, and the signal cycle approximately equal to the orbital period. In this paper, we could use the fourier series for modeling the low frequency error, achieve the high accuracy unity of AB and BC datum. The three component of Δ_{AB}^{BC} can be modeled by fourier function, and the compensation model of low frequency error is as follows:

$$\Delta_{\psi,k} = \sum_{j=1}^{M} \left[a_{\psi j} \cos(j\omega_0 k\tau) + b_{\psi j} \sin(j\omega_0 k\tau) \right]$$

$$\Delta_{\varphi,k} = \sum_{j=1}^{M} \left[a_{\varphi j} \cos(j\omega_0 k\tau) + b_{\varphi j} \sin(j\omega_0 k\tau) \right] \quad (1)$$

$$\Delta_{\theta,k} = \sum_{j=1}^{M} \left[a_{\theta j} \cos(j\omega_0 k\tau) + b_{\theta j} \sin(j\omega_0 k\tau) \right]$$

In which $\omega_0 = \dfrac{2\pi}{T}$ represents the angular frequency, T represents the satellite orbit period, k represents the number of time step, τ represents the time step, M is the normal number, $a_{\psi j}, b_{\psi j}, a_{\varphi j}, b_{\varphi j}, a_{\theta j}, b_{\theta j}$ indicates the unknown coefficient of low frequency error. We would construct the observation equation based on multi-circle observation data of low frequency error and the compensation model, the concrete form is as follows:

$$Z = \Phi X + V \quad (2)$$

In which Z represents sequence of low frequency error observation data, Φ represents observation matrix of fourier series model, X represents low frequency error coefficient of fourier series model, V represents model residuals. According to the least square principle, the optimal estimation $\hat{X}$ of the model coefficients of the low frequency error is obtained:

$$\hat{X} = (\Phi^T \Phi)^{-1} \Phi^T Z \quad (3)$$

Based on the above steps, the model construction of low frequency error can be realized, as well as the high accuracy unification of AB and BC attitude datum. Similarly, we could unify AC datum, and realize the unity of the whole internal datum.

2.3 External datum calibration and unifying

Due to the periodic variation of the satellite structure, the relationship between the star sensor and camera can also produce periodic changes, and we should carry out on orbit calibration of external absolute datum. Based on DOM/DEM reference data of the existing global geometric calibration field and the panchromatic image, we would use control points automatic measuring method and rigorous geometric imaging model to calculate attitude data of satellite body relative to J2000 coordinate system. The specific processing methods are as follows:

$$\begin{pmatrix} \tan(\psi_x(s)) \\ \tan(\psi_y(s)) \\ 1 \end{pmatrix} = \lambda R_{\text{body}}^{\text{cam}} \left(R_{\text{J2000}}^{\text{body}} R_{\text{wgs}}^{\text{J2000}} \begin{bmatrix} X_g - X_{\text{gps}} \\ Y_g - Y_{\text{gps}} \\ Z_g - Z_{\text{gps}} \end{bmatrix}_{\text{wgs}} - \begin{bmatrix} B_X \\ B_Y \\ B_Z \end{bmatrix}_{\text{body}} \right)$$

$$\begin{cases} \psi_x(s) = ax_0 + ax_1 \times s + ax_2 \times s^2 + ax_3 \times s^3 \\ \psi_y(s) = ay_0 + ay_1 \times s + ay_2 \times s^2 + ay_3 \times s^3 \end{cases}$$

$$(4)$$

Formula (4) represents a rigorous geometric imaging model based on the direction angle model of the probe element. In which (X_g, Y_g, Z_g) represents object square coordinates of object points; $(\psi_x(s), \psi_y(s))$ represents direction angle of probe element s; $(X_{gps}, Y_{gps}, Z_{gps})$ and (B_X, B_Y, B_Z) respectively represents object space coordinates of camera center and GPS eccentric error; λ represents a scaling factor; $R_{wgs}^{J2000}, R_{J2000}^{body}, R_{body}^{cam}$ respectively represents the rotation matrix of WGS84 coordinates to J2000 coordinates, J2000 coordinate system to the satellite body coordinate system and the satellite body coordinate system to the camera coordinate system. Further deduction of formula (4) is obtained:

$$\lambda^{-1}(R_{\text{body}}^{\text{cam}})^{-1}\begin{pmatrix}\tan(\psi_x(s)) \\ \tan(\psi_y(s)) \\ 1\end{pmatrix} = R_{\text{J2000}}^{\text{body}}R_{\text{wgs}}^{\text{J2000}}\begin{bmatrix}X_g - X_{\text{gps}} \\ Y_g - Y_{\text{gps}} \\ Z_g - Z_{\text{gps}}\end{bmatrix}_{\text{wgs}} - \begin{bmatrix}B_X \\ B_Y \\ B_Z\end{bmatrix}_{\text{body}} \quad (5)$$

The orbital data used in this paper is post precise orbit data, while the camera's internal calibration parameter is pointing angle model obtained by on-ground calibration results. With the line push broom camera, when a non-collinear observation vector on a matching control point in each scan line is ≥2, the attitude parameters along the scan line at certain time can be calculated from Eq.(5). In theory, to ensure the precision and reliability of the attitude parameters, a larger number of matching control points are required and they distribute evenly along the scan line. The attitude accuracy depends mainly on the accuracy of the GPS orbit accuracy, DEM/DOM accuracy of the reference calibration field data, and the number and distribution of the control points per scan line.

The attitude data obtained from the inversion method and attitude data of internal datum unification obtained in section 2.1 are aligned, and we will use the same method as section 2.1 to calculate the sequence of time-varying system error, construct the fourier series compensation model to obtain model parameters, and achieve the unity of external absolute datum.

3. EXPERIMENT AND DISCUSSION

3.1 Experimental data

Taking a certain type of high resolution optical satellite launched in December 2014 as an example, this paper will analyze and verify the effectiveness of low frequency error's on-ground compensation method. The satellite uses the sun synchronous orbit, and the orbit height is 490km. In order to enlarge the visible range of the earth observation camera, the satellite has the capability of side swing, the maximum side swing angle is $\pm45°$. The camera system composes of panchromatic camera and multi spectral camera. The nadir ground pixel resolution of panchromatic camera is 0.5 meters, as well as 2.0 meters for multi spectral camera. The data used in this paper is obtained during the satellite on orbit test.

3.2 Experimental results and analysis

(1) Low frequency error detection and analysis based on star sensor

When high resolution satellite is in process of push broom imaging, due to influence of space thermal environment, star sensor will appear thermal drift error, and the installation relationship between each other will change periodically. So we could detect the low frequency error based on star sensor's optical axis angle changes. The variation law of the optical axis angle error between A and B star sensor, A and C star sensor as well as B and C star sensor are respectively represented in Figures 1-3. What can be obtained by analyzing that the optical axis angle errors between each star sensor shows periodic variation with the orbital period, and optical axis angle error range of A and B star sensors is plus or minus 20 arcseconds, plus or minus 50 arcseconds of A and C, plus or minus 50 arcseconds of B and C.
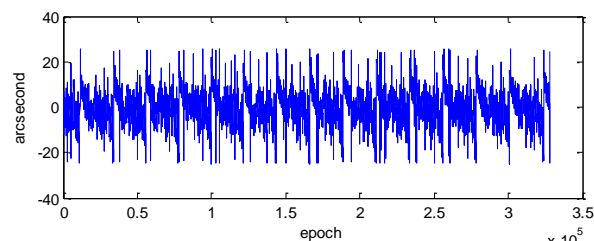

Figure 1. Chart of multiple orbits' A and B star sensor optical axis angle error change
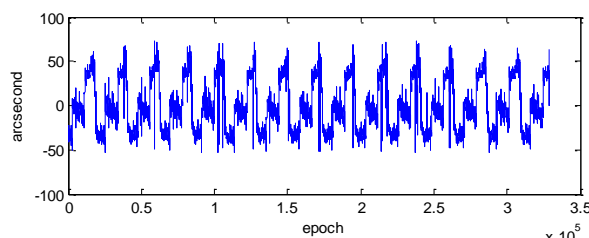

Figure 2. Chart of multiple orbits' A and C star sensor optical axis angle error change
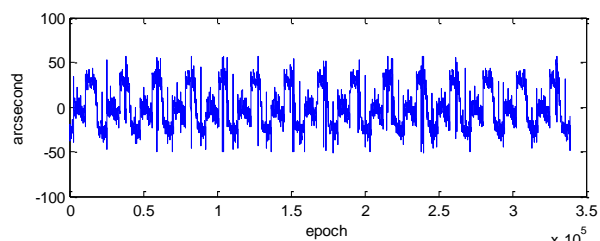

Figure 3. Chart of multiple orbits' B and C star sensor optical axis angle error change

The analysis results obtained from Figures 1-3 show that the thermal environment of space has made a certain degree of deformation on satellite structure, and the virtual datum determined by any of two star sensors has been changed periodically, which need to be calibrated for achieving consistency of internal datum.

(2) Analysis of internal relative datum's calibration results

The blue line of Figures 4-6 respectively represents on orbit calibration conversion parameters between virtual reference datum determined by AB star sensors and BC star sensors variation with the time, which performs in three directions of yaw, roll, pitch. The following conclusions are obtained from the analysis that the three directions of yaw, roll, pitch are changing periodically with orbital period, and the variation range of yaw angle is -10 ~ 5 arcseconds, -5 ~ 15 arcseconds for roll angle, -5 ~ 10 arcseconds for pitch angle.
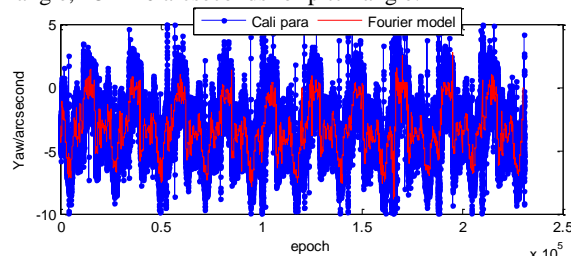

Figure 4. Chart of conversion parameters variation in yaw direction between AB and BC datum
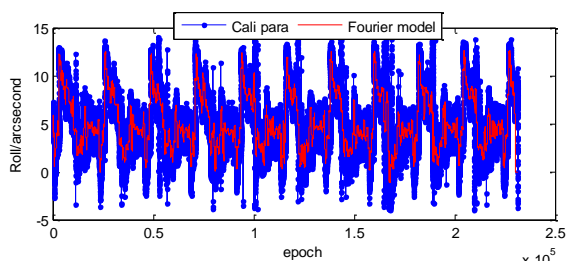
Figure 5. Chart of conversion parameters variation in roll direction between AB and BC datum
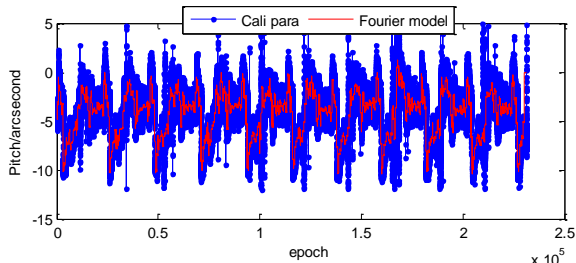

Figure 6. Chart of conversion parameters variation in pitch direction between AB and BC datum

The attitude maneuver needs to be done in advance when high-resolution optical satellite wants to take photos. In this process, when the star sensor meets the sun, it will automatically be shut down. So we would often meet the situation that only two star sensor or a single star sensor working. Switching of working mode of star sensors will inevitably lead to changes in the internal virtual datum, while the statistical results of Figures 4-6 can also show that there are differences in virtual datum determined by different star sensors, which needs for the unity of the internal datum. In this paper, we use the fourier series model to fit the conversion parameters between AB and BC virtual datum. The analysis results of Figures 4-6 show that the fitting results from the fourier series model are basically consistent with the on orbit calibration results, and the same principle could be used to model the conversion parameters between different virtual datum in other modes.

(3) Analysis of external absolute datum's calibration results
Space thermal environment will also affect the relationship between the star sensor and the camera. In this paper ,based on multi-orbits' attitude data of internal datum unification and large number of geometric calibration field image taken by camera and DOM/DEM image data, we could calculate the time series of conversion parameters between camera datum and internal datum. Figures 7-9 do analysis on the variation law of the conversion parameters between the internal datum and camera datum, research results show that the conversion parameters between the two datum also have the same periodic variation with the orbital period, and the variation range of yaw angle is 0 ~ 15 arcseconds, -20 ~ 10 arcseconds for roll angle, 10 ~ 40 arcseconds for pitch angle.
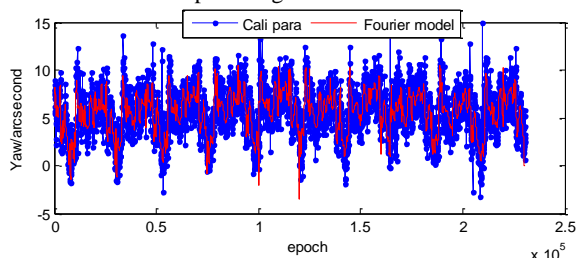

Figure 7. Chart of conversion parameters variation in yaw direction between internal and earth observation camera datum
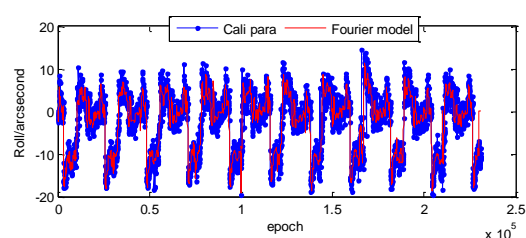

Figure 8. Chart of conversion parameters variation in roll direction between internal and earth observation camera datum
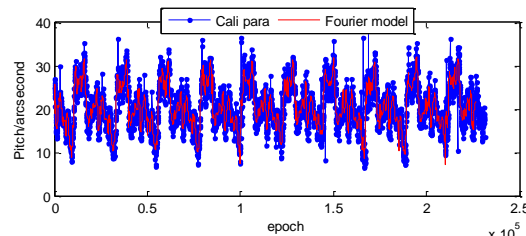

Figure 9. Chart of conversion parameters variation in pitch direction between internal and earth observation camera datum

In order to effectively eliminate the influence of the periodic variation of the conversion parameters between the internal datum and camera datum on the image geometric accuracy, this paper also uses the fourier series model to fit the conversion parameters, and the fitting results are consistent with the observed results. Table 1 and 2 respectively do statistics on geometry accuracy changes of panchromatic images before and after low frequency error compensation, and the statistical results show that the geometric positioning accuracy under no control point of panchromatic image is about 70 meters before low frequency error compensation, about 40 meters after compensating, and the overall results increases by about 40%. Therefore the low frequency error compensation method proposed in this paper can effectively improve the geometric positioning accuracy of high resolution optical image.

Time	Region	Positioning accuracy	RMS of offset	
			mdx	mdy
2015/5/30 11:24	Songshan	86.196	85.428	11.476
2015/7/13 13:41	Anyang	3.746	2.565	2.729
2015/7/17 13:35	Taiyuan	138.892	86.319	108.812
2015/7/21 13:29	Yili	73.528	53.362	50.585
2015/7/24 13:48	Dongying	15.190	14.361	4.950
2015/8/13 13:39	Sanya	81.509	56.161	59.073
2015/8/17 13:38	Lijiang	41.880	32.671	26.202
2015/8/18 13:14	Beijing	84.676	50.034	68.313
2015/8/21 13:37	Lasha	47.052	42.871	19.389

Table 1. Tables of geometric accuracy of panchromatic image when low frequency error compensation model is not added (Unit: meter)

Time	Region	Positioning accuracy	RMS of offset	
			mdx	mdy
2015/5/30 11:24	Songshan	58.311	58.020	5.816
2015/7/13 13:41	Anyang	3.819	2.461	2.920
2015/7/17 13:35	Taiyuan	17.843	12.877	12.352
2015/7/21 13:29	Yili	29.222	1.869	29.162
2015/7/24 13:48	Dongying	24.833	9.770	22.831
2015/8/13 13:39	Sanya	34.051	26.768	21.046
2015/8/17 13:38	Lijiang	27.374	11.765	24.716
2015/8/18 13:14	Beijing	77.244	50.062	58.825
2015/8/21 13:37	Lasha	40.414	4.631	40.148

Table 2. Tables of geometric accuracy of panchromatic image when low frequency error compensation model is added (Unit: meter)

4. CONCLUSIONS

Aiming at the current problems that high resolution remote sensing satellite image exists low frequency error and is difficult to be compensated, this paper proposes an algorithm of ground compensation method based on fourier series model, and does experimental analysis based on a high resolution optical satellite launched in December 2014, the research results show that: The low frequency error exists between different visual datum determined by different star sensor's combination; low frequency error also exists between the internal datum and the camera datum; the ground compensation method of calibrating the internal datum firstly, then calibrating the external datum could be used to improve the geometric positioning accuracy of high resolution optical image.

ACKNOWLEDGEMENTS

REFERENCES

Tang, X.M., Xie, J.F., 2011. Summary of high-resolution remote sensing satellite mapping key technology research. *2011 China Satellite Conference Proceedings*, Beijing, China Institute of Communications, pp. 182-191.

Li, D.R., Zhang, G., Jiang, Y.H., et al, 2016. Research on Image Geometric Precision of Domestic Optical Satellites. *Spacecraft Engineering*, 25(1), pp. 1-9.

Jin, T., Li, Z., Li, T., et al, 2013. System Design and Analysis for Improving Geometric Accuracy of High-Resolution Optical Remote Sensing Satellite Image. Journal of Astronautics, 34 (8), pp. 1160-1165.

Yuan, X.X., Yu, X., 2012. Calibration of Angular Systematic Errors for High Resolution Satellite Imagery. *Surveying and Mapping*, 41(3), pp. 386-392.

Bouillon, A., Bernard, M., Gigord, P., et al, 2006. SPOT 5 HRS geometric performances: using block adjustment as a key issue to improve quality of DEM generation. International Society for Photogrammetry and Remote Sensing, 60(3), pp. 134-146.

Digital G., 2009. WorldView-2 specifications,.http://www.digitalglobe.com/downloads/WorldView2-DS-WV2-Web.pdf.

Boulder C., 2016. Pleiades constellation capability overview, 2011. http://calval.cr.usgs.gov/JACIE_files/JACIE11/Presentations/WedPM/235_Stussi_JACIE_11.135.pdf.

Wang, D.B., Wang, Z.G., Tang, H.T., et al, 2014. GPS Based Orbit Determination Algorithm with High Precision and Low Computational Complexity for LEO Remote Sensing Satellites. *Chinese Space Science and Technology*, (2), pp. 54-61.

Sun, T., Xing, F., You, Z., 2013. Optical System Error Analysis of High Accuracy Star Trackers. *ACTA OPTICA SINICA,* 33(3), pp. 1-9.

Liu, H.B., Huang, S.H., Tan, J.C., et al, 2009. Thermo-optic Effects on Accuracy Performance of Star Tracker. *ACTA PHOTONICA SINICA*, 38(7), pp. 1836-1839.

Wang, J.Q., Xiong, K., Zhou, H.Y., 2012. Low-frequency Periodic Error Identification and Compensation for Star Tracker Attitude Measurement. *Chinese Journal of Aeronautics*, (25), pp. 615-621.

Xiong, K., Zong, H., Tang L., 2014. On Star Sensor Low Frequency Error In-Orbit Calibration Method. *Aerospace Control and Application*, 40(3), pp. 9-13.

Lam, Q., Woodruff, C., Ashton, S., et al, 2002. Noise estimation for star tracker calibration and enhanced precision attitude Determination. *Proceedings of the Fifth International Conference on Information Fusion*.

Morariu, V. I., Camps, O. I., 2006. Modeling Correspondences for Multi-Camera Tracking Using Nonlinear Manifold Learning and Target Dynamics. *IEEE Computer Society Conference on Computer Vision and Pattern Recognition*, pp. 545-552.

Sun, Y.H., 2014. Error analysis and calibration in star sensor application. Harbin: Harbin Institute of Technology.

Grodecki, J., Dial, G., 2003. Block adjustment of high-resolution satellite images described by rational polynomials. *Photogrammetric Engineering & Remote Sensing*, 69(1), pp. 59-68.

Toutin, T., 2004. Review article: Geometric processing of remote sensing images: models, algorithms and methods. *International Journal of Remote Sensing*, 25(10), pp. 1893-1924.